Int. J. Electrochem. Sci., 9 **(2014)** 5126 - 5154

International Journal of
ELECTROCHEMICAL
SCIENCE
www.electrochemsci.org

Thymus Vulgarise Extract as Nontoxic Corrosion Inhibitor for Copper and α-Brass in 1 M HNO_3 Solutions

A.S. Fouda[1,*], *K. Shalabi*[1], *A.A. Idress*[2]

[1]Department of Chemistry, Faculty of Science, Mansoura University, Mansoura-35516, Egypt
[2]Department of Chemistry, Faculty of Science, Omar Almukhtar University, Albayda, Libya
[*]E-mail: asfouda@hotmail.com

Received: 21 February 2014 / *Accepted:* 12 May 2014 / *Published:* 16 June 2014

The efficiency of Thymus vulgarise extract (TVE) as a nontoxic corrosion inhibitor for copper and α-brass in 1 M HNO_3 has been tested by weight loss and electrochemical techniques such as potentiodynamic polarization, electrochemical impedance spectroscopy (EIS) and electrochemical frequency modulation (EFM) techniques. The calculated adsorption thermodynamic parameters indicated that the adsorption was a spontaneous, exothermic process accompanied by a decrease in entropy. The inhibition efficiency increases with increasing the concentration of the extract in HNO_3 solution and decreases with increasing the temperature. The adsorption of the extract on the copper and α-brass surfaces in the acid solution was found to obey Langmuir's adsorption isotherm. Scanning electron microscope (SEM) results showed the formation of a protective film on the copper and α-brass surfaces in the presence of TVE. The results obtained from different techniques were in good agreement.

Keywords: Copper, α-Brass, Corrosion inhibition, Thymus Vulgarise, HNO_3, EIS, EFM, SEM, EDX.

1. INTRODUCTION

Copper is a metal that has a wide range of applications due to its good properties. It is used in electronics, for production of wires, sheets, tubes, and also to form alloys [1-3]. Copper is easily combined with many metals. It forms with zinc brasses, which have a higher corrosion resistance and a very easy manufacture. Moreover, brasses are harder and solid. However, their exhibition in acid media creates problems of corrosion [4-8]. When the brasses, containing more than 15% of zinc, are exposed in corrosive environments, they are affected not only by general corrosion damage, but also by dezincification process involving preferential dissolution of zinc, leaving a spongy mass of copper on the alloy surface [9].

The use of copper corrosion inhibitors in acid solutions is usually to minimize the corrosion of copper during the acid cleaning and descaling. The possibility of the copper corrosion prevention has attracted many researchers so until now numerous possible inhibitors have been investigated [10-12]. The inhibiting action of these inhibitors is attributed to their adsorption to the metal/solution interface. It has been observed that adsorption depends mainly on certain physico-chemical properties of the inhibitor group. Like functional groups, aromaticity, electron density at the donor atoms and π-orbital character of donating electrons and also the presence of hetero-atom such as N, O and S, as well as multiple bonds in their molecular structure, are assumed to be active centers of adsorption [13].

But the toxicity of most corrosion inhibitors made us heading for the use of environment-friendly inhibitors [14].

Plant extract is low-cost and environmental safe, so the main advantages of using plant extracts as corrosion inhibitor are economic and safe environment. Up till now, many plant extracts have been used as effective corrosion inhibitors for copper in acidic media, such as: Zenthoxylum alatum [15], Azadirachta Indica [16], caffeine [17] Cannabis[18]. The inhibition performance of plant extract is normally ascribed to the presence of complex organic species, including tannins, alkaloids and nitrogen bases, carbohydrates and proteins as well as hydrolysis products in their composition. These organic compounds usually contain polar functions with nitrogen, sulfur, or oxygen atoms and have triple or conjugated double bonds with aromatic rings in their molecular structures, which are the major adsorption centers.

Thyme (Thymus Vulgarise), a member of the lamiaceae family, is an aromatic and has medicinal plant properties [19]. This plant is indigenous to the Mediterranean region of Europe and is extensively cultured in the United States. Known primary constituents of the thyme include essential oil, tannin, flavonoids, saponins, and triterpenic acid [20]. Its volatile phenolic oil has been reported to be among the top 10 essential oils, showing antibacterial, antimycotic, anti oxidative, natural food preservative and mammalian age delaying properties [19]

The aim of this paper is to study the action of TVE as non toxic corrosion inhibitor for copper and α-brass in 1 M HNO_3 solution using different techniques. The surface morphology of copper and α-brass were studied by scanning electron microscope (SEM) and energy dispersive X-ray (EDX) techniques.

2. EXPERIMENTAL

2.1. Materials and solutions

Experiments were performed using copper specimens (99.98%) and α-brass (60-40 copper-zinc) were mounted in Teflon. An epoxy resin was used to fill the space between Teflon and copper and also α-brass electrode. The aggressive solution used was prepared by dilution of analytical reagent grade 70% HNO_3 with bidistilled water. The stock solution (2000 ppm) of TVE was used to prepare the desired concentrations by dilution with bidistilled water. The concentration range of TVE used was 50-300 ppm.

2.2. Preparation of plant extracts

Fresh aerial parts of Thymus Vulgarise were collected from green mountain, Libya, in spring (June 2013). The Plant materials of Thymus Vulgarise were shade dried at room temperature for 13 days. The shade dried plant materials were crushed to make fine powder. The powdered materials (100 g each) were soaked in 250 ml of methanol for 5 days and then subjected to repeated extraction with 25× 30 ml until exhaustion of plant materials. The extracts obtained were then concentrated under reduced pressure using rotary evaporator at temperature below 55°C. The methanol evaporated to give solid extract that was prepared for application as corrosion inhibitor.

2.3. Weight loss measurements

The samples used were machined to be a rectangular (2 x 2 x 0.30 cm). Polishing of the samples was done mechanically with speed polisher. The samples were polished with emery paper up to grade 1200 grit size. After being polished they were rinsed in acetone, dried, and wrapped in filter paper. The samples were rinsed in distilled water and wiped dry before immersing them in the test solution.

After weighting accurately, the specimens were immersed in 100 ml of 1 M HNO_3 with and without different concentration of TVE at 25 – 45 $^{\circ}$C. After different immersion time (30, 60, 90, 120, 150 and 180 min) the copper coupons were taken out, washed with distilled water then dried and weighted accurately. The inhibition efficiency (IE %) and the degree of surface coverage (Θ) were calculated from:

$$\%IE = \theta \times 100 = \left(1 - \frac{W_{(inh)}}{W_{(free)}}\right) \times 100 \quad (1)$$

where, W_{free} and W_{inh} are the weight loss in the absence and presence of inhibitor, respectively.

2.3. Electrochemical measurements

All the electrochemical measurements were performed using the electrochemical workstation (Gamry PCI4-G750 Instruments) and a constant temperature of 25 ± 1 $^{\circ}$C is maintained in the acid medium. Prior to the electrochemical measurements, all samples were prepared according to the procedure described above. The platinum electrode and saturated calomel electrode (SCE) were used as auxiliary and reference electrodes, respectively. The working electrodes constitute copper or α-brass specimens of 1 cm^2 area. The tip of the reference electrode is positioned very close proximity to the working electrode surface by the use of fine Luggin capillary in order to minimize ohmic potential drop. Remaining uncompensated resistance was also reduced by electrochemical workstation. Each experiment was repeated at least three times to check the reproducibility.

Potentiodynamic polarization studies were carried out at a scan rate of 1 mV s^{-1}. The electrode potential was allowed to stabilize for 30 min until a constant potential was reached, which is referred as the OCP. In all the cases, OCP was established first, and then the polarization experiment was carried out. The polarization curves for copper specimens in the test solution with and without various

concentrations of inhibitors were recorded from -1000 to 1200 mV at open circuit potential. Then i_{corr} was used for the calculation of inhibition efficiency and surface coverage (θ) as below [21]:

$$\%IE = \theta \times 100 = \left(1 - \frac{i_{corr(inh)}}{i_{corr(free)}}\right) \times 100 \quad (2)$$

The electrochemical impedance studies were carried out in the same setup used for potentiodynamic polarization studies described above. We applied the ac perturbation signal of 10 mV within the frequency range of 100 kHz to 0.2 Hz. All electrochemical impedance measurements were carried out at open circuit potential. The efficiency of the inhibition and the surface coverage (θ) obtained from the impedance measurements are defined by the following relations:

$$\% IE = \theta \times 100 = \left(1 - \left[\frac{R^{\circ}_{ct}}{R_{ct}}\right]\right) \times 100 \quad (3)$$

where R°_{ct} and R_{ct} are the charge transfer resistance in the absence and presence of inhibitor, respectively.

Electrochemical frequency modulation, EFM, was carried out using two frequencies of 2 and 5 Hz. The base frequency was 0.1 Hz, so that the wave form repeats after 1 s. The intermodulation spectra contain current responses assigned for harmonical and intermodulation current peaks. The larger peaks were used to calculate the corrosion current density (i_{corr}), the Tafel slopes (β_c and β_a) and the causality factors CF-2 & CF-3[22].

2.4. Surface examination

The surface films were formed on the copper specimens by immersing them in inhibitor solutions for a period of 24 h. After the immersion period, the specimens were taken out, dried and the nature of the film formed on the surface of the metal specimen was analyzed by EDX and SEM techniques. Examination of copper and α-brass surface after 24 h exposure to the 1 M HNO_3 solution without and with inhibitor was carried out by Hitachi S-550 Scanning Electron Microscope. Rough elemental analyses for the exposed surface were conducted by EDX technique.

3. RESULTS AND DISCUSSION

3.1. Weight loss measurements

Weight loss measurements were carried out in 1 M HNO_3 in the absence and presence of different concentrations of TVE and are shown in Figures (1, 2). Corrosion rates of copper and α-brass in (mg cm^{-2} min^{-1}) and the inhibition efficiency (IE %) were calculated using equation (1). The average corrosion rates, expressed in (mg cm^{-2} min^{-1}), are shown in Tables 1. The results show that TVE used inhibit the corrosion copper and α-brass in 1 M HNO_3 solutions. The corrosion rate was found to depend on the concentration of the TVE. Increasing the concentration of each TVE increases the inhibition efficiency IE% which reached its maximum value at concentration of 300 ppm for the copper and α-brass. This indicates that the protective effect of TVE is not solely due to their reactivity with the nitric acid. The inhibitory behavior of these compounds against copper and α-brass corrosion

can be attributed to the adsorption of TVE on the copper and α-brass surface, which limits the dissolution of the latter by blocking of their corrosion sites and hence decreasing the corrosion rate, with increasing efficiency as their concentrations increase [23].

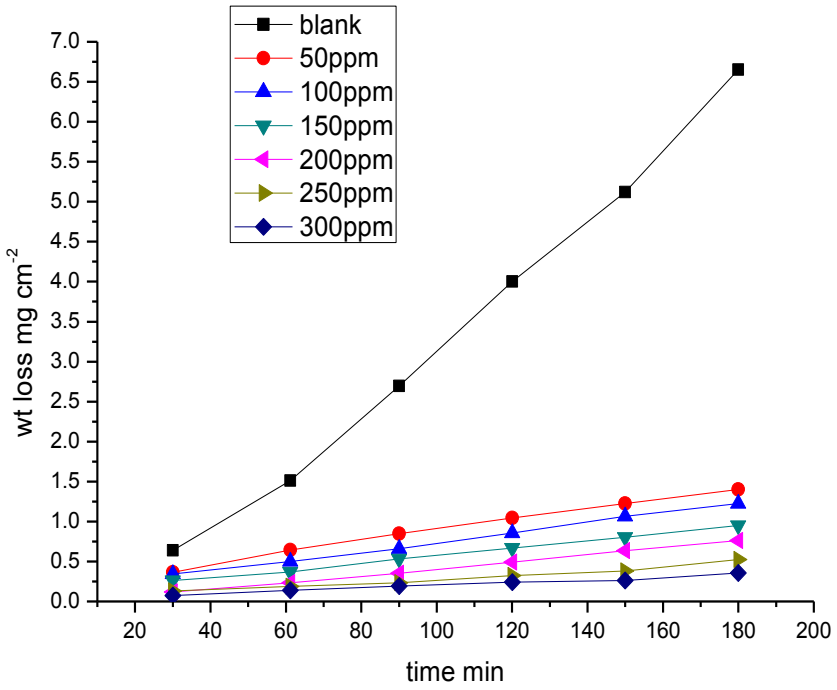

Figure 1. Weight loss-time curves for the corrosion of copper in 1 M HNO_3 in the absence and presence of different concentrations of Thymus vulgarise at 25°C

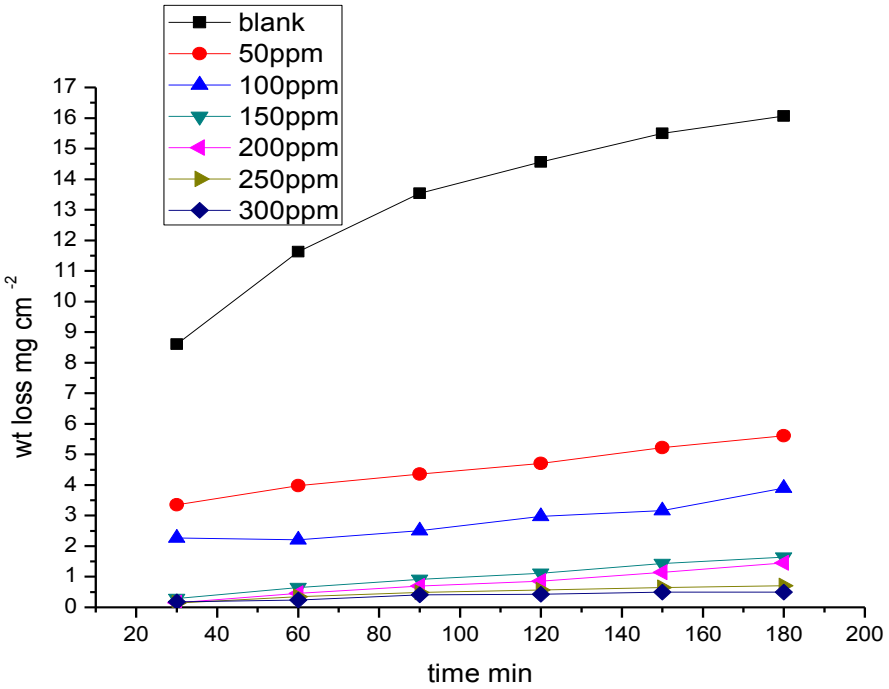

Figure 2. Weight loss-time curves for the corrosion of α-brass in 1 M HNO_3 in the absence and presence of different concentrations of Thymus vulgarise at 25°C.

Table 1. Corrosion rate (C.R.) in (mg cm^{-2} min^{-1}) and inhibition efficiency data obtained from weight loss measurements for copper and α-brass in 1 M HNO_3 solutions without and with various concentrations of TVE at 25°C

	Conc., ppm	Weight loss, mg/cm^2	C.R., mg cm^{-2} min^{-1}	θ	%IE
Copper	1 M HNO_3	4.00351	0.0333	-	-
	50	1.04564	0.0087	0.787	73.9
	100	0.8553	0.0071	0.787	78.7
	150	0.66769	0.0056	0.833	83.3
	200	0.4899	0.0041	0.878	87.8
	250	0.3216	0.0027	0.920	92.0
	300	0.24232	0.0020	0.939	93.9
α-Brass	1 M HNO_3	14.5625	0.1214	-	-
	50	4.70588	0.0392	0.677	67.7
	100	2.97629	0.0248	0.800	80.0
	150	1.11443	0.0093	0.921	92.1
	200	0.85982	0.0072	0.941	94.1
	250	0.56892	0.0047	0.960	96.0
	300	0.424	0.0035	0.970	97.0

3.1.1. Effect of temperature and activation Parameters of Corrosion Process

The effect of temperature, in the range of 25–45°C with an increment of 5 °C on both the corrosion rate (C.R.) and the inhibition efficiency of different TVE concentrations in each of 1 M HNO_3 was studied by weight loss measurements and was given in Tables (2, 3).

Table 2. Data of weight loss measurements for copper in 1 M HNO_3 solution in the absence and presence of different concentrations of Thymus vulgarise at 25–45°C.

Conc., ppm	Temp., °C	C.R., mg$cm^{-2}min^{-1}$	θ	IE%
50	25	0.0087	0.739	**73.9**
	30	0.0215	0.511	**51.1**
	35	0.0344	0.357	**35.7**
	40	0.0599	0.265	**26.5**
	45	0.0802	0.117	**11.7**
100	25	0.0071	0.787	**78.7**
	30	0.0153	0.652	**65.2**
	35	0.0285	0.466	**46.6**
	40	0.0459	0.443	**44.3**
	45	0.0706	0.223	**22.3**
150	25	0.0056	0.833	**83.3**
	30	0.0142	0.677	**67.7**
	35	0.0238	0.555	**55.5**
	40	0.0404	0.509	**50.9**
	45	0.0605	0.334	**33.4**

200	25	0.0041	0.878	**87.8**
	30	0.0119	0.729	**72.9**
	35	0.0215	0.598	**59.8**
	40	0.0327	0.603	**60.3**
	45	0.0514	0.435	**43.5**
250	25	0.0027	0.920	**92.0**
	30	0.0105	0.761	**76.1**
	35	0.0186	0.652	**65.2**
	40	0.0288	0.650	**65.0**
	45	0.0446	0.510	**51.0**
300	25	0.0020	0.939	**93.9**
	30	0.0085	0.806	**80.6**
	35	0.0142	0.734	**73.4**
	40	0.0248	0.699	**69.9**
	45	0.0371	0.591	**59.1**

Table 3. Data of weight loss measurements for brass in 1 M HNO_3 solution in the absence and presence of different concentrations of Thymus vulgarise at 25–45°C

Conc., ppm	**Temp; °C**	**CR($mgcm^{-2}min^{-1}$)**	**θ**	**IE%**
50	25	0.039216	0.677	**67.6**
	30	0.134914	0.481	**48.1**
	35	0.272461	0.348	**34.8**
	40	0.521771	0.221	**22.1**
	45	0.598542	0.179	**17.9**
100	25	0.024802	0.800	**80.0**
	30	0.092186	0.645	**64.5**
	35	0.178666	0.573	**57.3**
	40	0.336952	0.497	**47.9**
	45	0.432397	0.407	**40.7**
150	25	0.009287	0.921	**92.1**
	30	0.043996	0.831	**83.1**
	35	0.101649	0.757	**75.7**
	40	0.199792	0.701	**70.1**
	45	0.223003	0.694	**69.4**
200	25	0.007165	0.941	**94.1**
	30	0.015979	0.938	**93.8**
	35	0.031546	0.924	**92.4**
	40	0.068957	0.897	**89.7**
	45	0.120769	0.834	**83.4**
250	25	0.004741	0.960	**96.0**
	30	0.012174	0.953	**95.3**
	35	0.02151	0.948	**94.8**
	40	0.041352	0.938	**93.8**
	45	0.064033	0.9122	**91.22**
300	25	0.003533	0.970	**97.0**
	30	0.010467	0.959	**95.9**
	35	0.020961	0.950	**95.0**
	40	0.037131	0.944	**94.4**
	45	0.057041	0.921	**92.1**

From Tables (3, 4); we can see that increasing the temperature leads to an increase in the corrosion rate of copper and α-brass both in free acid and inhibited acid solution and a decrease in the inhibition efficiency of the extract which suggested that corrosion inhibition of copper by the investigated compounds caused by the adsorption of inhibitor molecule while higher temperatures caused the desorption of the extract components from the copper surface [24].

The apparent activation energy E_a^*, enthalpy of activation ΔH^*, and entropy of activation ΔS^* for the corrosion of samples in 1 M HNO_3 solution in the absence and presence of different concentrations of the plant extract at 25-45°C were calculated from Arrhenius-type equation:

$$Rate = A\, e^{\frac{-E_a^*}{RT}} \quad (4)$$

and transition-state equation:

$$Rate = \frac{RT}{Nh}\, e^{\frac{\Delta S^*}{R}}\, e^{\frac{-\Delta H^*}{RT}} \quad (5)$$

where A is the frequency factor, h is Planck's constant, N is Avogadro's number, and R is the universal gas constant. A plot of log rate vs. 1/T and log (rate/T) vs. 1/T give straight lines with slope of - E_a^*/2.303R and ΔH^*/2.303R, respectively. The intercept will be A and log (R/Nh) + (ΔS^*/2.303R) for Arrhenius and transition state equations, respectively.

Figures (3, 4) represent plots of log rate vs. 1/T and Figures (5, 6) represent plots of log (rate/T) vs. 1/T data. The calculated values of the apparent activation energies, E_a^*, activation entropies, ΔS^*, and activation enthalpies, ΔH^*, are given in Table 5. The almost similar values of E_a^* suggest that the inhibitors are similar in the mechanism of action. Also, the values of activation energy E_a^* increase in the same order of increasing inhibition efficiency of the inhibitor. It is also indicated that the whole process is controlled by surface reaction, since the energy of activation corrosion process is over 20 kJ mol^{-1} **[**25**].**

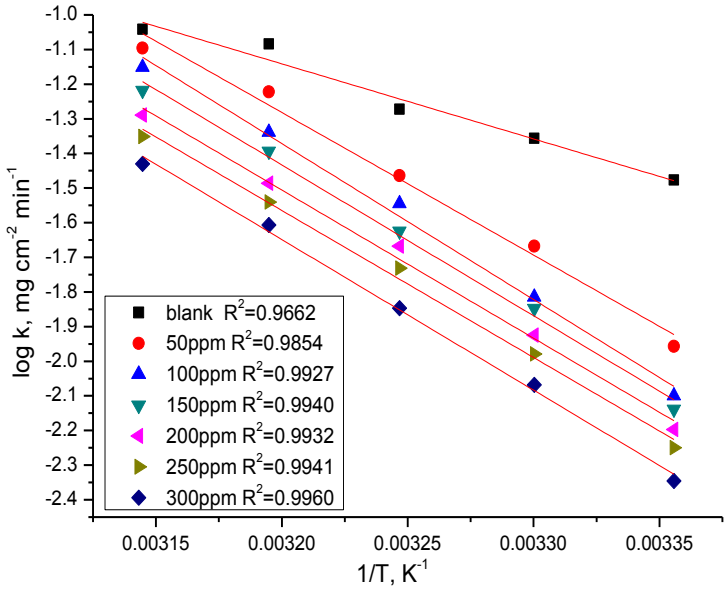

Figure 3. Log corrosion rate - 1/T curves for copper dissolution in 1M HNO_3 in absence and presence of different concentrations of TVE

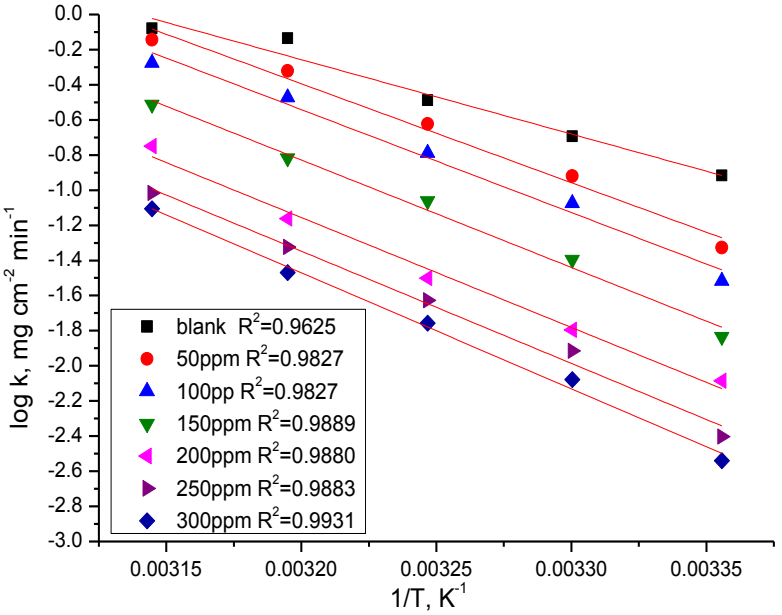

Figure 4. Log corrosion rate - 1/T curves for α-brass dissolution in 1 M HNO_3 in absence and presence of different concentrations of TVE

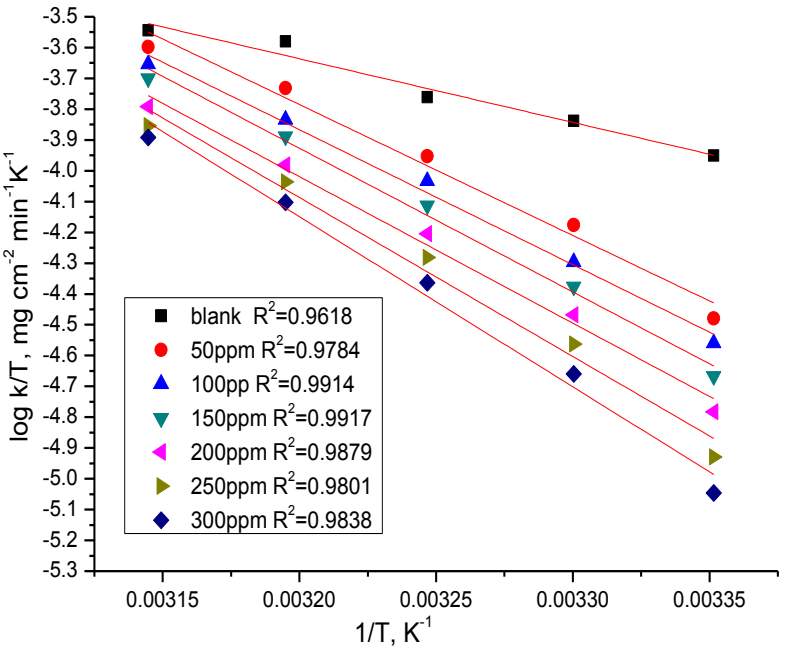

Figure 5. Log (corrosion rate/T)-(1/T) curves for copper dissolution in 1 M HNO_3 in absence and presence of different concentrations of TVE

From the results of Table 5, it is clear that the presence of the plant extract increased the activation energy values and consequently decreased the corrosion rate of the copper and brass. Also, activation energy increased by increasing the concentration of the extract. These results indicate that

this tested compound acted as inhibitors through increasing activation energy of copper dissolution by making a barrier to mass and charge transfer by their adsorption on copper surface.

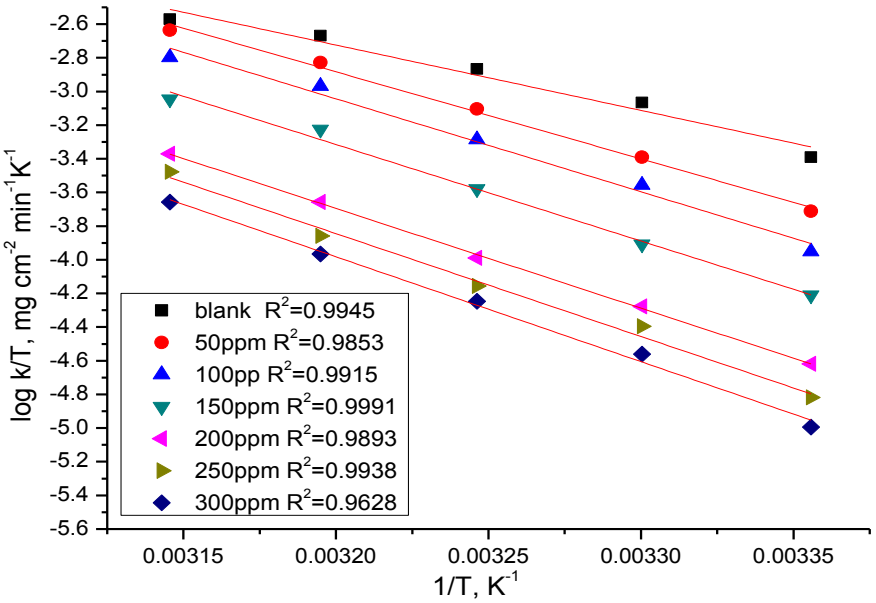

Figure 6. Log (corrosion rate/T)-(1/T) curves for α-brass dissolution in 1M HNO_3 in absence and presence of different concentrations of TVE

Table 4. Effect of concentration of TVE on the activation energy of copper and α-brass dissolution in 1 M HNO_3

		Activation parameters		
	Conc., ppm	E_a^* kJ mol $^{-1}$	ΔH^* kJ mol $^{-1}$	ΔS^* J mol^{-1} K^{-1}
Copper	1 M HNO_3	41.49	39.56	-140.63
	50	78.83	81.42	-9.52
	100	86.23	88.45	-11.35
	150	83.38	89.34	-13.13
	200	81.92	91.08	-16.93
	250	81.28	98.84	-40.46
	300	83.27	105.73	-61.31
α-Brass	1 M HNO_3	81.05	74.40	-11.64
	50	107.85	99.04	-64.14
	100	112.19	105.71	-82.42
	150	117.10	109.78	-90.24
	200	119.77	113.49	-94.85
	250	122.29	117.05	-103.36
	300	126.35	119.28	-107.87

The increase in the activation enthalpy (ΔH^*) in the presence of the inhibitors implies that the addition of the inhibitors to the acid solution increases the height of the energy barrier of the corrosion reaction to an extent depends on the type and concentration of the present inhibitor [26]. The entropy of activation (ΔS^*) is large and negative, which implies that the activated complex represents association rather than dissociation step. Accordingly, this indicates that a decrease in disorder takes place, going from reactants to the activated complex [27].

3.1.2. Adsorption isotherm

Organic molecules inhibit the corrosion process by the adsorption on metal surface. Theoretically, the adsorption process can be regarded as a single substitutional process in which an inhibitor molecule (Inh.) in the aqueous phase substitutes an "x" number of water molecules adsorbed on the metal surface [28] vis,

$$Inh(aq.) + xH_2O(sur) \text{ ----------} \rightarrow Inh(sur.) + xH_2O(aq.) \quad (6)$$

where x is known as the size ratio and simply equals the number of adsorbed water molecules replaced by a single inhibitor molecule. The adsorption depends on the structure of the inhibitor, the type of the metal and the nature of its surface, the nature of the corrosion medium and its pH value, the temperature, and the electrochemical potential of the metal-solution interface. Also, the adsorption provides information about the interaction among the adsorbed molecules themselves as well as their interaction with the metal surface. Actually an adsorbed molecule may make the surface more difficult or less difficult for another molecule to become attached to a neighboring site and multilayer adsorption may take place. There may be more or less than one inhibitor molecule per surface site. Finally, various surface sites could have varying degrees of activation.

A number of mathematical relationships for the adsorption isotherms have been suggested to fit the experiment data of the present work.

The degree of surface coverage (θ), i.e, the fraction of the surface covered by the inhibitor molecules at any given concentration of the inhibitor, was calculated from the equation mentioned % IE = (100x θ). The values of θ have been shown in Tables (2, 3). The degree of surface coverage was found to increase with increasing concentration of the extract. Attempts were made to fit θ values to various isotherms including Langmuir, Freundlich, Temkin and Frumkin. By far, the best fit was obtained with Langmuir isotherm.

The equilibrium constant of the adsorption process, K, which is related to the standard free energy of adsorption ($\Delta G°_{ads}$) by [29, 30]:

$$\frac{\theta}{1-\theta} = KC \quad (7)$$

$$K = \frac{1}{55.5} e^{\frac{-\Delta G^{\circ}_{ads}}{RT}} \quad (8)$$

where 55.5 is the concentration of water molecule in (mol L^{-1}) at metal/solution interface.

Figures (7, 8) show the plot of θ /1- θ vs. C for different concentrations of the extract. This plot gives straight line with slope very close to unity. The regression (R^2) is more than 0.9. This means that there is no interaction between the adsorbed species on the electrode surface [31].

All the calculated thermodynamic parameters are listed in Table 5. The negative value of $\Delta G°_{ads}$ in Table 5 suggested that the adsorption of inhibitor molecules on to copper and α-brass surface is spontaneous process. Generally, values of $\Delta G°_{ads}$ up to -20 kJ mol^{-1} are consistent with electrostatic interaction between the charged molecules and the charged metal (physical adsorption) while those more negative than -40 kJ mol^{-1} involve charge sharing or transfer of electrons from the inhibitor molecules to the metal surface to form a coordinate type of bond (chemisorption) [32, 33].

Moreover, the adsorption heat can be calculated according to the Van't Hoff equation 9 [34]:

$$\ln K = -\frac{\Delta H^{o}_{ads}}{RT} + const \quad (9)$$

Figure 9 show the plot of log vs. 1/T for copper and brass dissolution in 1 M HNO_3 in the presence of TVE. The $\Delta H°_{ads}$ values (Table 5) are negative, which show that the adsorption is an exothermic process [35].

Finally, the standard adsorption entropy $\Delta S°_{ads}$ can be calculated by the equation 10:

$$\Delta S^{o}_{ads} = \frac{\Delta H^{o}_{ads} - \Delta G^{o}_{ads}}{T} \quad (10)$$

The $\Delta S°_{ads}$ values (Table 5) are negative, which show that the adsorption is an exothermic process and always accompanied by a decrease of entropy. The reason can be explained as follows: the adsorption of organic inhibitor molecules from the aqueous solution. Table 5 lists all the above calculated thermodynamic parameters [36-37].

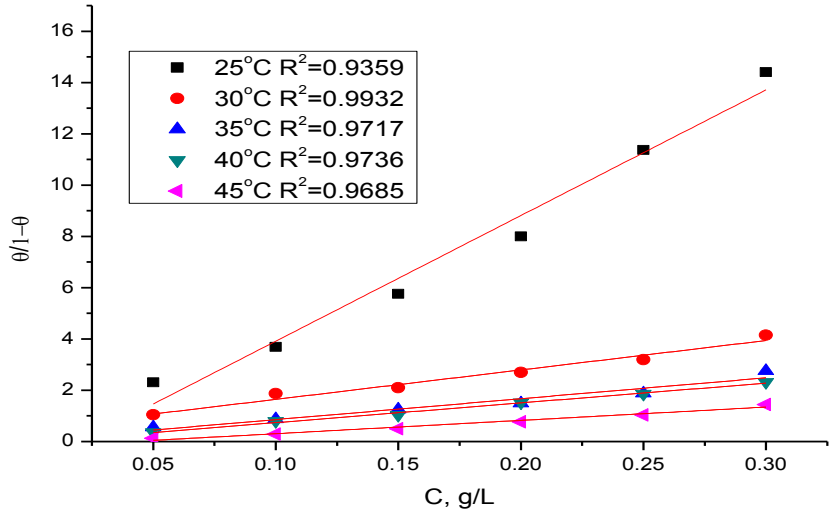

Figure 7. Adsorption isotherm curves for the adsorption of TVE on copper in 1 M HNO_3 at different temperatures

Table 5. Thermodynamic parameters for copper and α-brass in 1 M HNO_3 for TVE at 25-45°C

	Temp., K	K_{ads}, $g^{-1}l$	$\Delta G°_{ads}$, kJ mol^{-1}	$\Delta H°_{ads}$, kJ mol^{-1}	$\Delta S°_{ads}$, J mol^{-1} K^{-1}
Copper	298	50.62	-19.68	-82.20	-275.83
	303	11.47	-16.27		-271.28

	308	8.15	-15.66		-266.87
	313	7.70	-15.77		-262.61
	318	5.19	-14.98		-258.48
α-Brass	298	123.13	-21.88	-32.50	-109.062
	303	101.74	-21.77		-107.26
	308	86.88	-21.72		-105.52
	313	75.23	-21.70		-103.84
	318	50.89	-21.01		-102.20

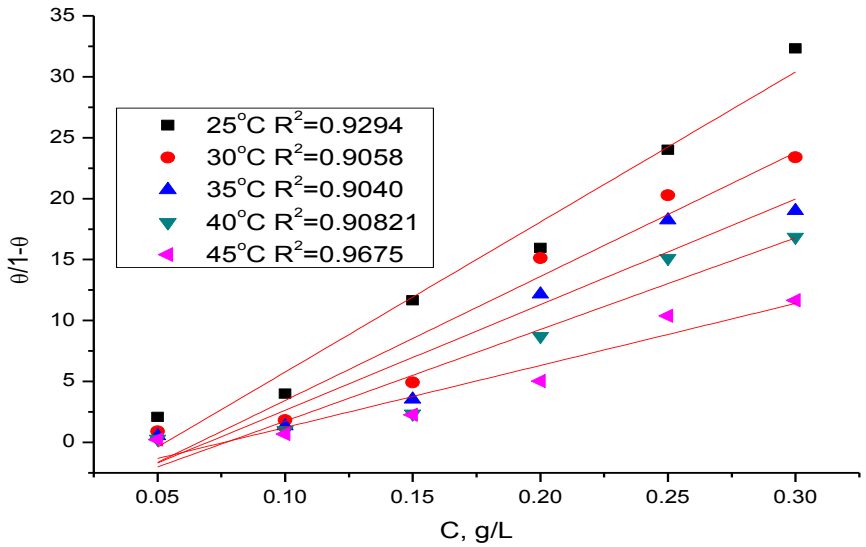

Figure 8. Adsorption isotherm curves for the adsorption of TVE on α-brass in 1 M HNO_3 at different temperatures

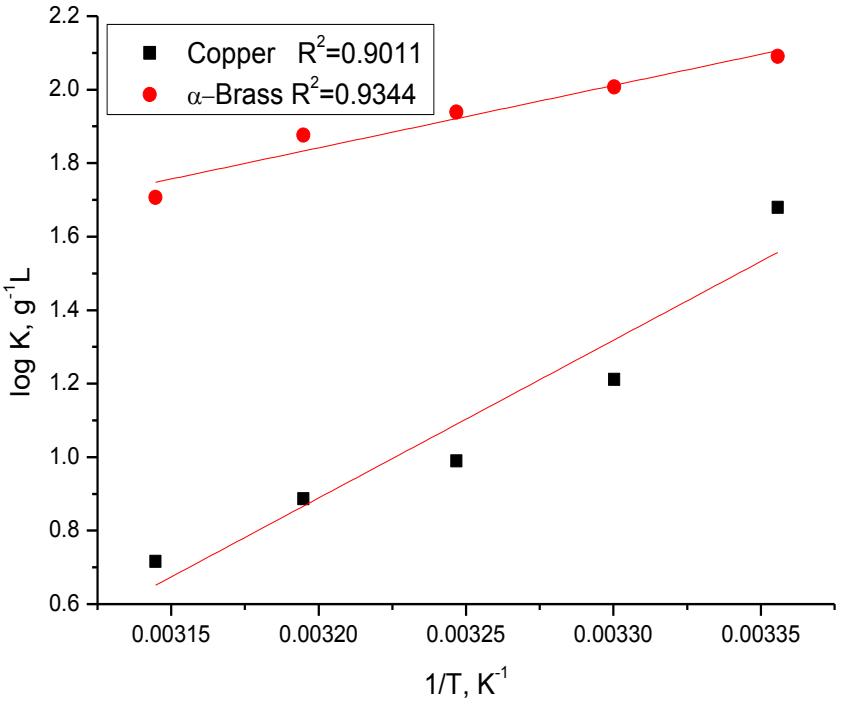

Figure 9. Log K vs. (1/T) curves for copper and α- brass dissolution in 1 M HNO_3 in the presence of TVE

3.2. Polarization Curves

Copper can hardly be corroded in the deoxygenated acid solutions, as copper cannot displace hydrogen from acid solutions according to the theories of chemical thermodynamics [38-39].

Potentiodynamic polarization technique is based on current and potential measurements. It is generally accepted that the inhibitor molecule inhibits corrosion by adsorbing at the metal/solution interface.

Figures (10, 11) show typical polarization curves for copper and brass in 1 M HNO_3 media. The two distinct regions that appeared were the active dissolution region (apparent Tafel region), and the limiting current region. In the inhibitor-free solution, the anodic polarization curve of copper showed a monotonic increase of current with potential until the current reached the maximum value. After this maximum current density value, the current density declined rapidly with potential increase, forming an anodic current peak that was related to Cu $(NO_3)_2$ film formation. In the presence of TVE, both the cathodic and anodic current densities were greatly decreased over a wide potential range from (-1 to 1.3 V vs. SCE). Various corrosion parameters such as corrosion potential ($E_{corr.}$), anodic and cathodic Tafel slopes (β_a, β_c), the corrosion current density (i_{corr}), the degree of surface coverage (θ) and the inhibition efficiency (%IE) are given in Table 6.

It can see from the experimental results that in all cases, addition of inhibitors induced a significant decrease in cathode and anodic currents. The values of E_{corr} were affected and slightly shifted to more negative direction by the addition of inhibitors. The lower values of i_{corr} in the presence of investigated extract without causing significant changes in E_{corr} values and suggest that TVE extract is mixed type mainly cathodic for copper and brass.

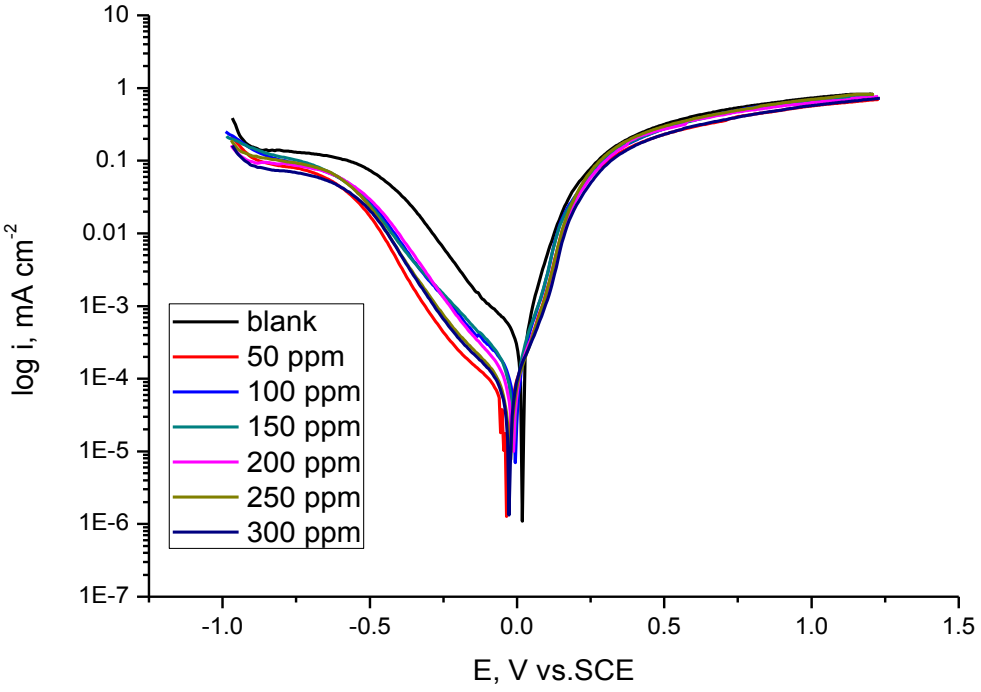

Figure 10. Potentiodynamic polarization curves for the corrosion of copper in 1 M HNO_3 solution without and with various concentrations of TVE at 25˚C.

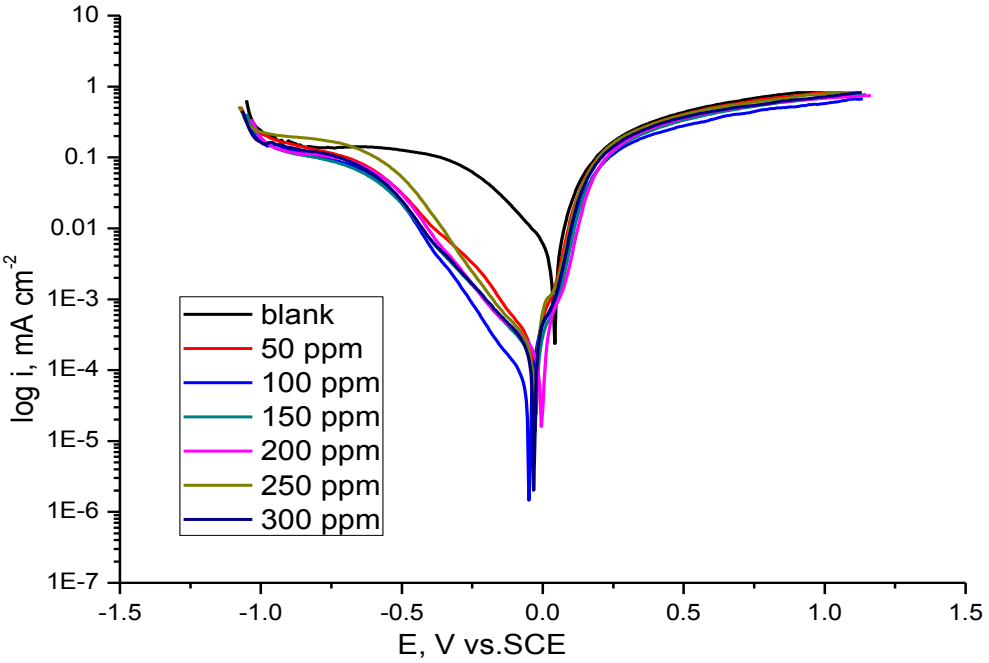

Figure 11. Potentiodynamic polarization curves for the corrosion of α-brass in 1 M HNO_3 solution without and with various concentrations of TVE at 25˚C

Table 6. Effect of concentration of TVE on the electrochemical parameters calculated from potentiodynamic polarization technique for the corrosion of copper and α-brass in 1 M HNO_3 at 25˚C

Conc., ppm		i_{corr}, μA cm^{-2}	$-E_{corr}$, mV vs. SCE	β_a, $Vdec^{-1}$	β_c, $Vdec^{-1}$	CR, mp y^{-}	θ	%IE
Copper	1 M HNO_3	379.0	17.60	102.2	221.7	173.0	---	---
	50	170.0	-11.20	114.4	238.1	77.79	0.551	55.1
	100	118.0	-4.520	85.40	218.3	53.68	0.689	68.9
	150	103	-14.20	100.3	204.3	46.85	0.728	72.8
	200	62.9	-23.90	90.20	194.6e	28.74	0.834	83.4
	250	55.4	-26.20	92.00	192.7	25.30	0.854	85.4
	300	41.70	-34.80	90.50	192.8	19.06 y	0.89	89.00
α-Brass	1 M HNO_3	1860.0	50.30	95.20	346.3	921.2	---	---
	50	426.0	-25.40	107.1	268.9	211.4	0.771	77.1
	100	294.0	-30.30	98.80	227.4	146.0	0.842	84.2
	150	209	-26.20	97.20	247.9	103.5	0.888	88.8
	200	176.0	-32.30	86.40	226.4	87.09	0.905	90.5
	250	169.0	-37.60	81.30	236.7	84.01	0.909	90.9
	300	79.70	-48.20	84.00	196.5	39.54	0.957	95.7

3.3. Electrochemical impedance spectroscopy (EIS)

EIS is well-established and powerful technique in the study of corrosion. Surface properties, electrode kinetics and mechanistic information can be obtained from impedance diagrams [40-44]. Figures (12,14), Figures (13,15) show the Nyquist and Bode plots obtained at open-circuit potential both in the absence and presence of increasing concentrations of TVE at room temperature. The increase in the size of the capacitive loop with the addition of TVE shows that a barrier gradually forms on the copper surface. From the Bode plots the total impedance increases with inhibitor concentration (log Z vs. log f). But (log f vs. phase) from Bode plot shows the continuous increase in the phase angle shift, obviously correlating with the increase of inhibitor adsorbed on Cu surface. The Nyquist plots do not yield perfect semicircles as expected from the theory of EIS. The deviation from ideal semicircle was generally attributed to the frequency dispersion [45] as well as to the in homogeneities of the surface.

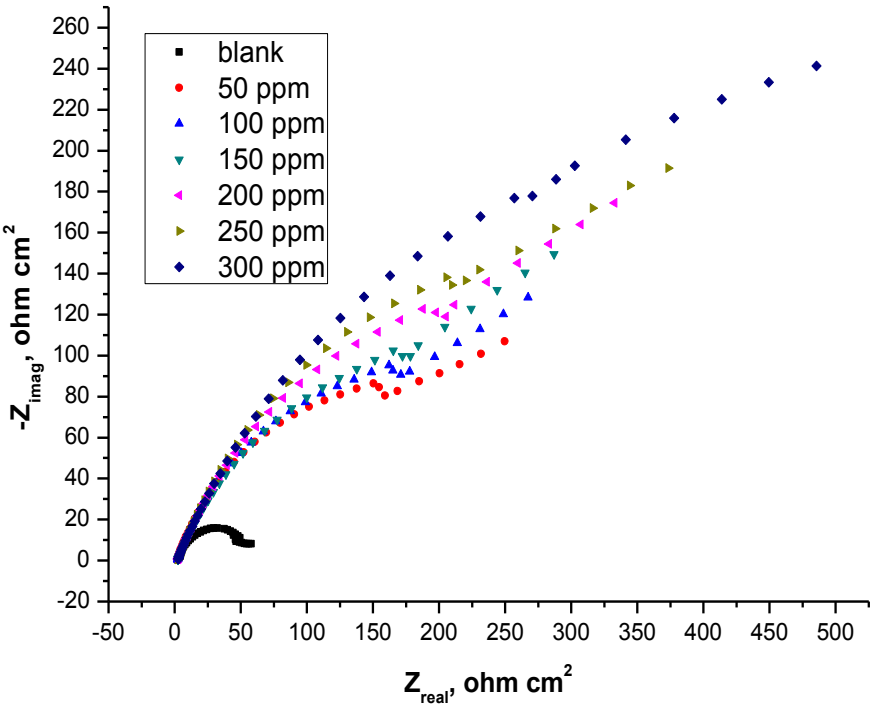

Figure 12. Nyquist plots recorded for copper in 1 M HNO_3 without and with various concentrations of TVE at 25±1˚C.

EIS spectra of the these compounds were analyzed using the equivalent circuit in Figure 16, where R_s represents the solution resistance, R_{ct} denotes the charge-transfer resistance, and a CPE instead of a pure capacitor represents the interfacial capacitance [46]. The impedance of a CPE is described by the following equation:

$$Z_{CPE} = Y_0^{-1}(j\omega_{max})^{-n} \quad (11)$$

where Y_0 is the magnitude of the CPE, j is an imaginary number, ω is the angular frequency ($\omega_{max} = 2\pi f_{max}$), f_{max} is the frequency at which the imaginary component of the impedance reaches its

maximum values, and n is the deviation parameter of the CPE: $-1 \leq n \leq 1$. The values of the interfacial capacitance C_{dl} can be calculated from CPE parameter values Y_0 and n using equation 11 [47]:

$$C_{dl} = Y_0(\omega_{max})^{n-1} \quad (12)$$

After analyzing the shape of the Nyquist plots, it is concluded that the curves approximated by a single capacitive semicircles, showing that the corrosion process was mainly charged-transfer controlled [48, 49]. The general shape of the curves is very similar for all samples (in presence or in absence of inhibitors at different immersion times) indicating that no change in the corrosion mechanism [50]. From the impedance data (Table 7), we conclude that the value of R_{ct} increases with increase in concentration of the inhibitors and this indicates an increase in % IE.

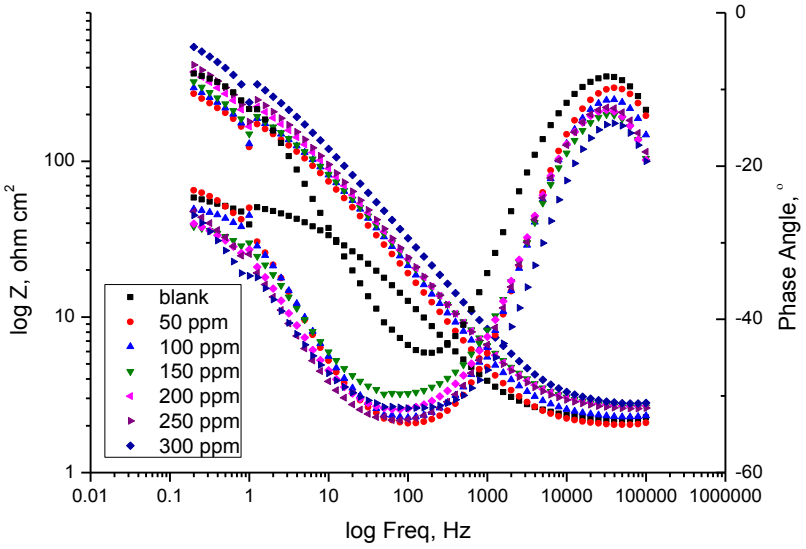

Figure 13. Bode plots recorded for copper in 1 M HNO_3 without and with various concentrations of TVE at 25±1˚C.

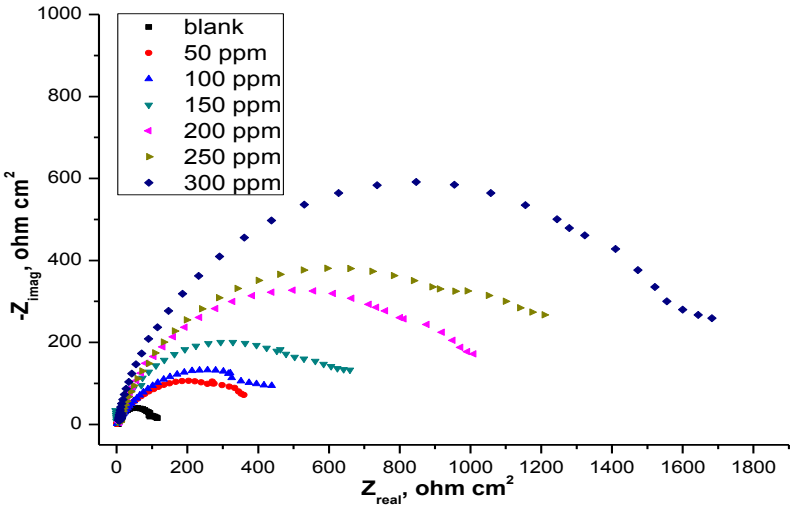

Figure 14. Nyquist plots recorded for brass in 1 M HNO_3 without and with various concentrations of TVE at 25±1°C.

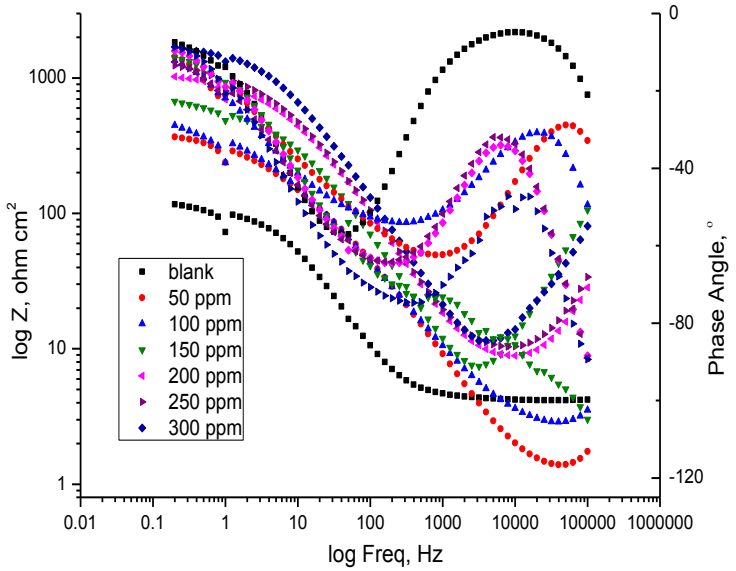

Figure 15. Bode plots recorded for brass in 1 M HNO_3 without and with various concentrations of TVE at 25±1˚C.

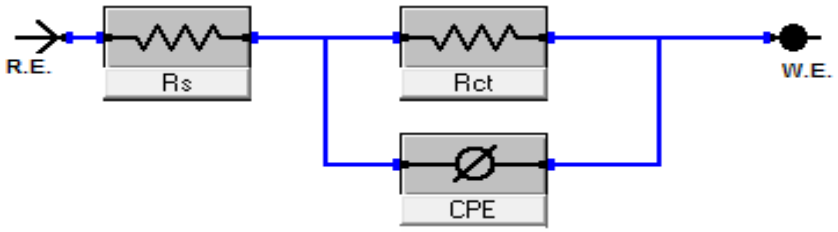

Figure 16. Electrical equivalent circuit used to fit the impedance data

Table 7. Electrochemical kinetic parameters obtained from EIS technique for copper and brass in 1 M HNO_3 solution containing various concentrations of TVE at 25˚C

	Conc., ppm,	R_{ct}, Ω cm^2	C_{dl}, µF cm^{-2}	θ	%IE
Copper	1 M HNO_3	53.51	270.0	--	--
	50	262.90	58.4	0.796	79.6
	100	294.40	54.2	0.808	80.8
	150	377.40	47.9	0.858	85.8
	200	429.60	42.3	0.875	87.5
	250	460.00	37.6	0.884	88.4
	300	668.60	35.4	0.920	92.0
α-Brass	1 M HNO_3	102.10	280.9	--	--
	50	357.42	46.2	0.714	71.4
	100	450.50	41.1	0.773	77.3
	150	700.11	37.2	0.854	85.4
	200	999.44	34.9	0.898	89.8
	250	1200.59	32.7	0.915	91.5
	300	1679.33	28.9	0.939	93.9

The presence of inhibitors enhances the value of R_{ct} in acidic solution for copper and brass. Values of double layer capacitance are also brought down to the maximum extent in the presence of inhibitor and the decrease in the values of CPE follows the order similar to that obtained for i_{corr} in this study. The decrease in CPE/C_{dl} results from a decrease in local dielectric constant and/or an increase in the thickness of the double layer, suggesting that TVE extract inhibit the copper corrosion by adsorption at metal/acid [51, 52].

3.4. Electrochemical frequency modulation technique (EFM)

Electrochemical frequency modulation is a nondestructive corrosion measurement technique that can directly give values of the corrosion current without prior knowledge of Tafel constants. Like EIS, it is a small ac signal. Unlike EIS, however, two sine waves (at different frequencies) are applied to the cell simultaneously. Because current is a non-linear function of potential, the system responds in a nonlinear way to the potential excitation. The current response contains not only the input frequencies, but also contains frequency components which are the sum, difference, and multiples of the two input frequencies. The two frequencies may not be chosen at random. They must both be small, integer multiples of a base frequency that determines the length of the experiment.

The great strength of the EFM is the causality factors which serve as an internal check on the validity of EFM measurement. The causality factors CF-2 and CF-3 are calculated from the frequency spectrum of the current responses. Figures(17a, 18a) show the frequency spectrum of the current response of pure copper and brass in nitric acid solution, contains not only the input frequencies, but also contains frequency components which are the sum, difference, and multiples of the two input frequencies. The EFM intermodulation spectrums of copper and brass in nitric acid solution containing (50ppm- 300ppm) of the TVE extract at 25±1°C are shown in Figures (17b-g, 18b-g). The harmonic and intermodulation peaks are clearly visible and are much larger than the background noise. The two large peaks, with amplitude of about 200 μA, are the response to the 40 and 100 mHz (2 and 5 Hz) excitation frequencies. It is important to note that between the peaks there is nearly no current response (<100 mA). The experimental EFM data were treated using two different models: complete diffusion control of the cathodic reaction and the "activation" model. For the latter, a set of three non-linear equations had been solved, assuming that the corrosion potential does not change due to the polarization of the working electrode. The larger peaks were used to calculate the corrosion current density (i_{corr}), the Tafel slopes (β_c and β_a) and the causality factors (CF-2 and CF-3). These electrochemical parameters were simultaneously determined by Gamry EFM140 software, and listed in Table 8 indicating that this extract inhibit the corrosion of copper in 1 M HNO_3 through adsorption. The causality factors obtained under different experimental conditions are approximately equal to the theoretical values (2 and 3) indicating that the measured data are verified and of good quality [53]. The inhibition efficiencies IE_{EFM} % increase by increasing the studied extract concentrations for either copper or α-brass and was calculated as follows:

$$IE\ \%_{EFM} = \left(1 - \frac{i_{corr}}{i_{corr}}\right) \times 100 \quad (13)$$

where i^{o}_{corr} and i_{corr} are corrosion current densities in the absence and presence of EHE extract, respectively.

3.5. SEM/EDX examination

In order to verify if the TVE molecules are in fact adsorbed on copper and α-brass surface, both SEM and EDX experiments were carried out. The SEM micrographs for copper and α-brass surface alone and after 24 h immersion in HNO_3 without and with the addition of 300 ppm of TVE are shown in Figures (19a-c, 20a-c). The corresponding EDX profile analyses are presented in Figures (21, 22). As expected, Figures (19a, 20 a) shows metallic surface is clear, while in the absence of the TVE, the copper and α-brass surface is damaged by HNO_3 corrosion (Figures (19b, 20b). In contrast, in presence of the TVE (Figures (19c, 20c)), the metallic surface seems to be almost no affected by corrosion. The corresponding EDX data are presented in Figures (21, 22) and Table 9. It is clear from the EDX spectra of copper and α-brass in the presence of TVE, the existence of C and O peaks (Figures(21,22) which suggest the adsorption of TVE on the copper and α-brass surface and confirm the formation of a thin film of TVE observed in SEM micrograph, thus protecting the surface against corrosion.

3.6. Mechanism of inhibition

Most organic inhibitors contain at least one polar group with an atom of nitrogen or sulphur or in some cases selenium and phosphorus. The inhibiting properties of many compounds are determined by the electron density at the reaction center [54].

With increase in electron density in the center, the chemisorption between the inhibitor and the metal are strengthened [56, 57].The plant extract TVE is composed of numerous naturally occurring organic compounds. Accordingly, the inhibitive action of TVE could be attributed to the adsorption of its components on the copper surface. The constituents of TVE are phytochemical constituents is essential oil (borneol, carvacrol, cymol, linalool, and thymol), tannin, flavonoids (apigenin and luteolin), saponins, and triterpenic acid [58, 20]. Its volatile phenolic oil has been reported to be among the top 10 essential oils. Most of these phytochemicals are organic compounds that have center for π-electron and presence of hetero atoms such as oxygen and nitrogen; hence, the adsorption of the inhibitor on the surface on copper is enhanced by their presence. The inhibition efficiency of methanol extracts of TVE is due to the formation of multi-molecular layer of adsorption between copper and some of these phytochemicals. Results of the present study have shown that TVE inhibits the acid induced corrosion of copper by virtue of adsorption of its components onto the metal surface. The inhibition process is a function of the metal, inhibitor concentration, and temperature as well as inhibitor adsorption abilities, which is so much dependent on the number of adsorption sites. The mode of adsorption observed could be attributed to the fact that TVE contains many different chemical compounds some of it are protonated in the acid medium and others do not, the protonated ones are adsorbed electrostatically with the metal and alloy surfaces. This observation may derive the fact that adsorbed organic molecules can influence the behaviour of electrochemical reactions involved in

corrosion processes in several ways. The action of organic inhibitors depends on the type of interactions between the substance and the metallic surface. The interactions can bring about a change either in electrochemical mechanism or in the surface available for the processes [59].

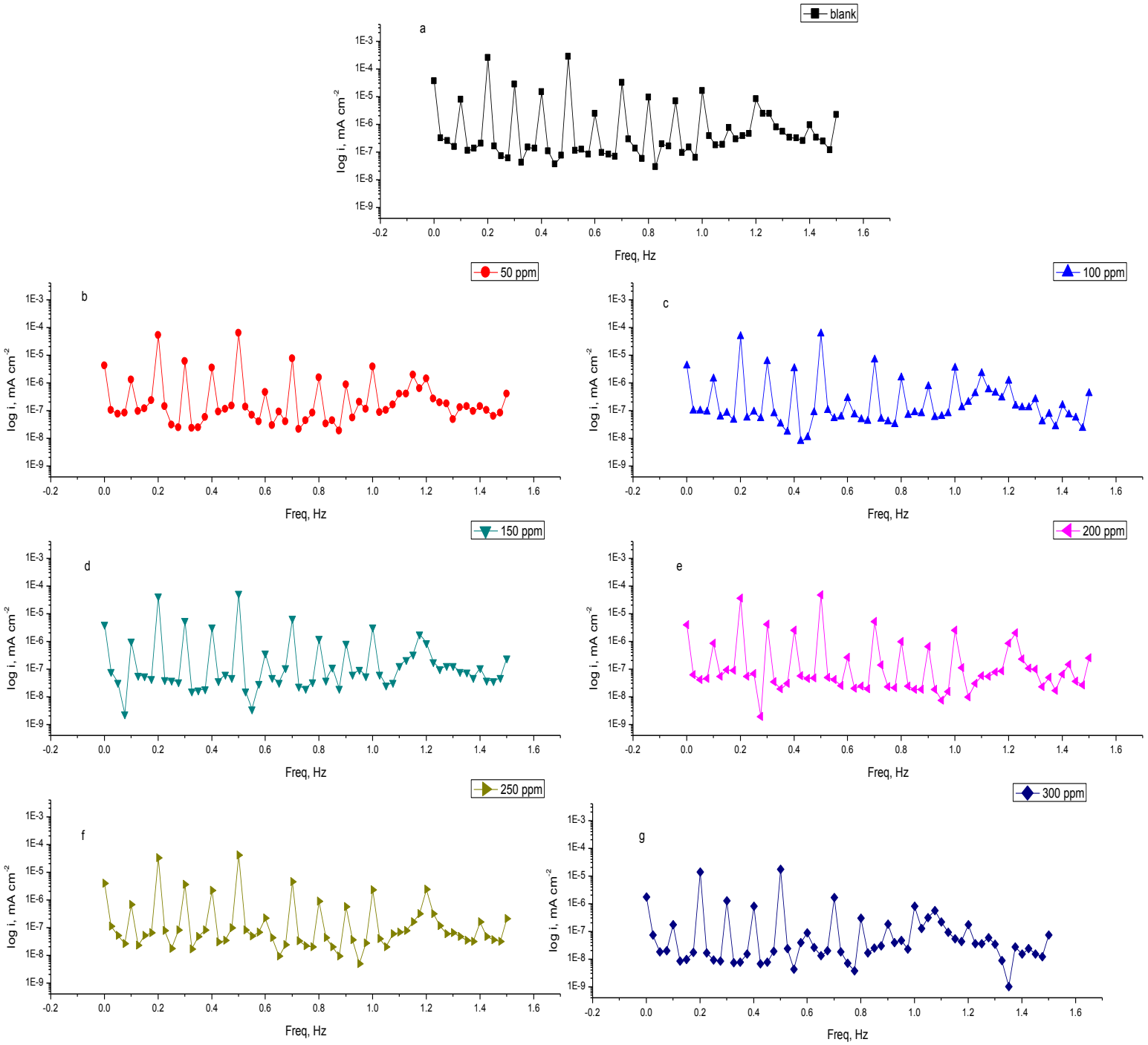

Figure 17(a-g). Intermodulation spectrums for the corrosion of copper in 1 M HNO_3 without and with various concentrations of TVE at 25˚C

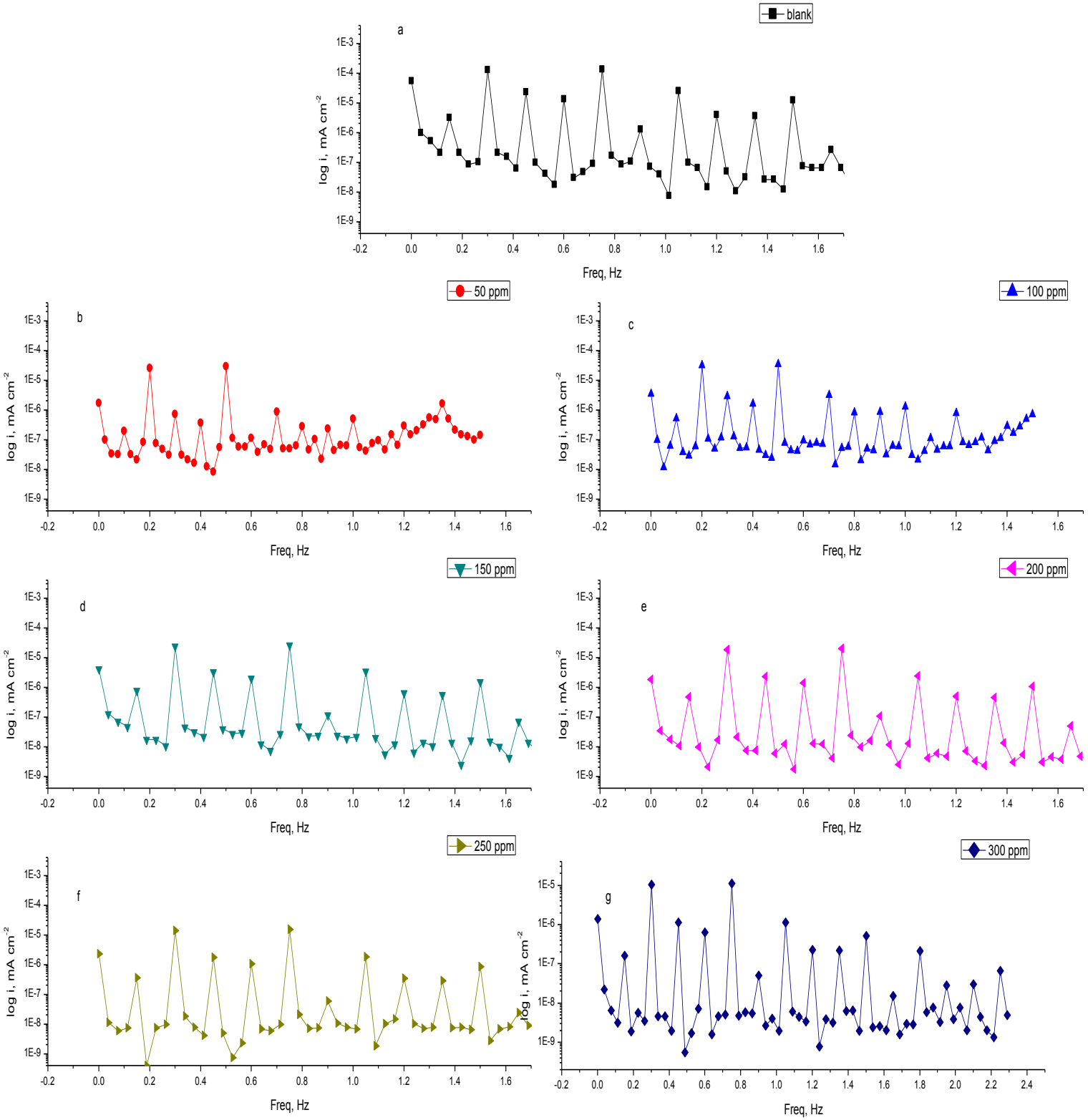

Figure 18(a-g). Intermodulation spectrums for the corrosion of α-brass in 1 M HNO_3 without and with various concentrations of TVE at 25˚C

Table 8. Electrochemical kinetic parameters obtained by EFM technique for copper and brass in 1 M HNO_3 solution containing different concentrations of TVE at 25˚C

	Conc., ppm	i_{corr}, μA cm^{-2}	β_a, $mVdec^{-1}$	β_c, $mVdec^{-1}$	CR, mm y^{-1}	CF-2	CF-3	θ	%IE
Copper	1 M HNO_3	291.1	57	95	143.70	1.96	3.44	----	----
	50	77.7	66.810	126	38.36	1.83	2.99	0.733	73.3
	100	73.07	67	126	36.06	1.91	3.51	0.749	74.9
	150	71.9	69	150	35.49	1.86	3.14	0.753	75.3
	200	61	71	138	30.10	1.86	3.14	0.791	79.1
	250	41.41	57	94	20.44	1.83	3.22	0.858	85.8
	300	28.3	86	125	13.91	1.84	2.54	0.903	90.3
α-Brass	1 M HNO_3	199.3	63	215	98.33	1.88	2.94	----	----
	50	51	65	138	25.17	1.83	1.95	0.744	74.4
	100	42	67	107	21.29	2.04	1.88	0.789	78.9
	150	33	63	134	16.28	1.92	4.36	0.834	83.4
	200	25	64	123	12.34	1.92	3.62	0.875	87.5
	250	21	68	141	10.36	1.92	3.93	0.895	89.5
	300	16	73	137	7.90	1.95	3.46	0.920	92.0

4. CONCLUSIONS

From the overall experimental results the following conclusions can be deduced:

1. TVE is good inhibitor and act as mixed type but mainly cathodic inhibitors for copper and brass corrosion in 1 M HNO_3 solution.

2. The results obtained from chemical measurements showed that the inhibiting action increases with the inhibitor concentration and decreases with the increasing in temperature.

3. Double layer capacitances decrease with respect to blank solution when the plant extract is added. This fact confirms the adsorption of plant extract molecules on the copper and brass surfaces.

4. The adsorption of inhibitor on copper and brass surfaces in HNO_3 solution follows Langmuir isotherm for TVE.

5. The negative values of the free energy of adsorption and adsorption heat are indicate that the process was spontaneous and exothermic.

6. The values of inhibition efficiencies obtained from the different independent quantitative techniques used show the validity of the results.

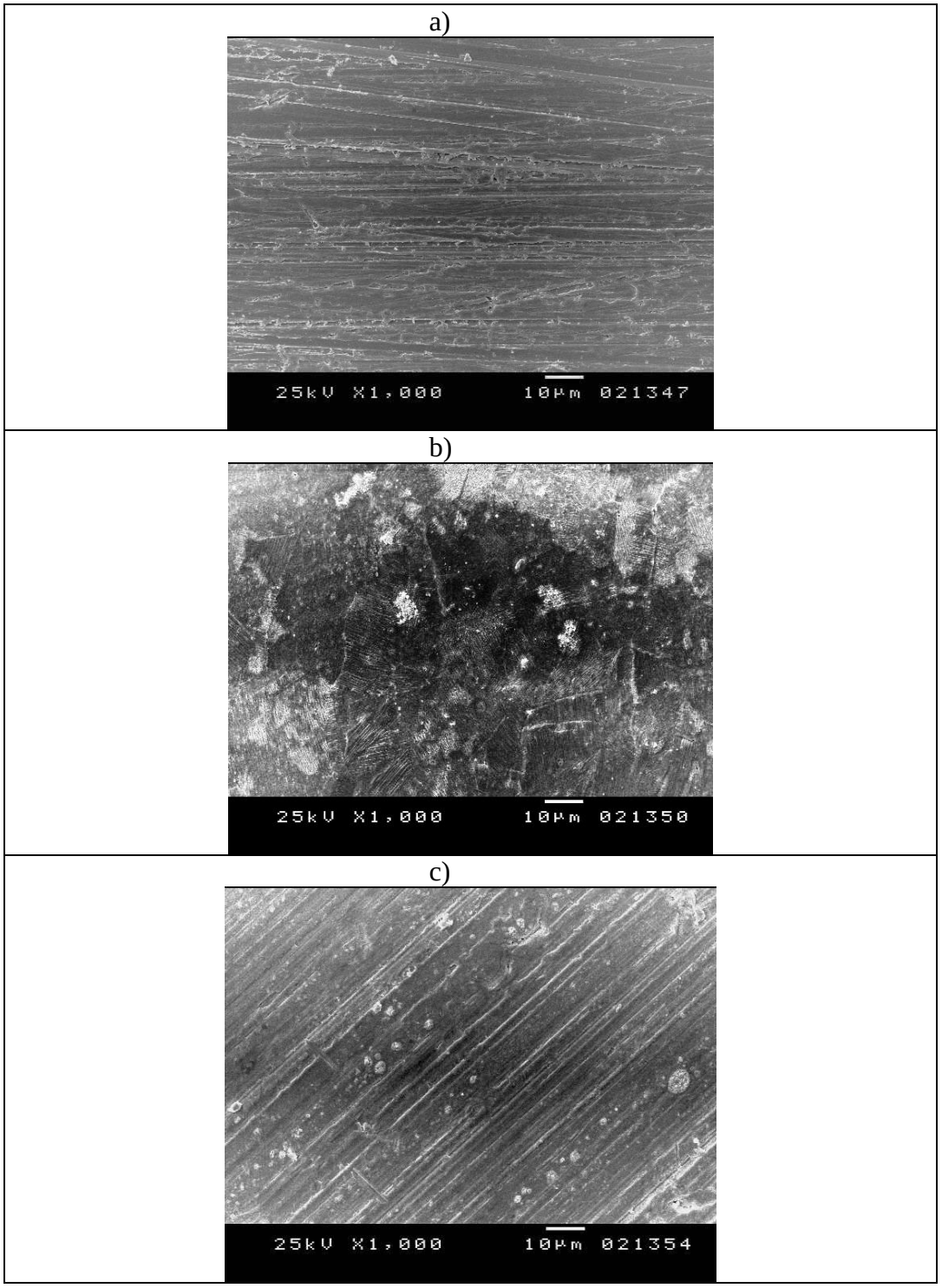

Figure 19. SEM micrographs of copper surface (a) before of immersion in 1 M HNO_3, (b) after 24 h of immersion in 1 M HNO_3 and (c) after 24 h of immersion in 1 M HNO_3+ 300 ppm TVE at 25°C

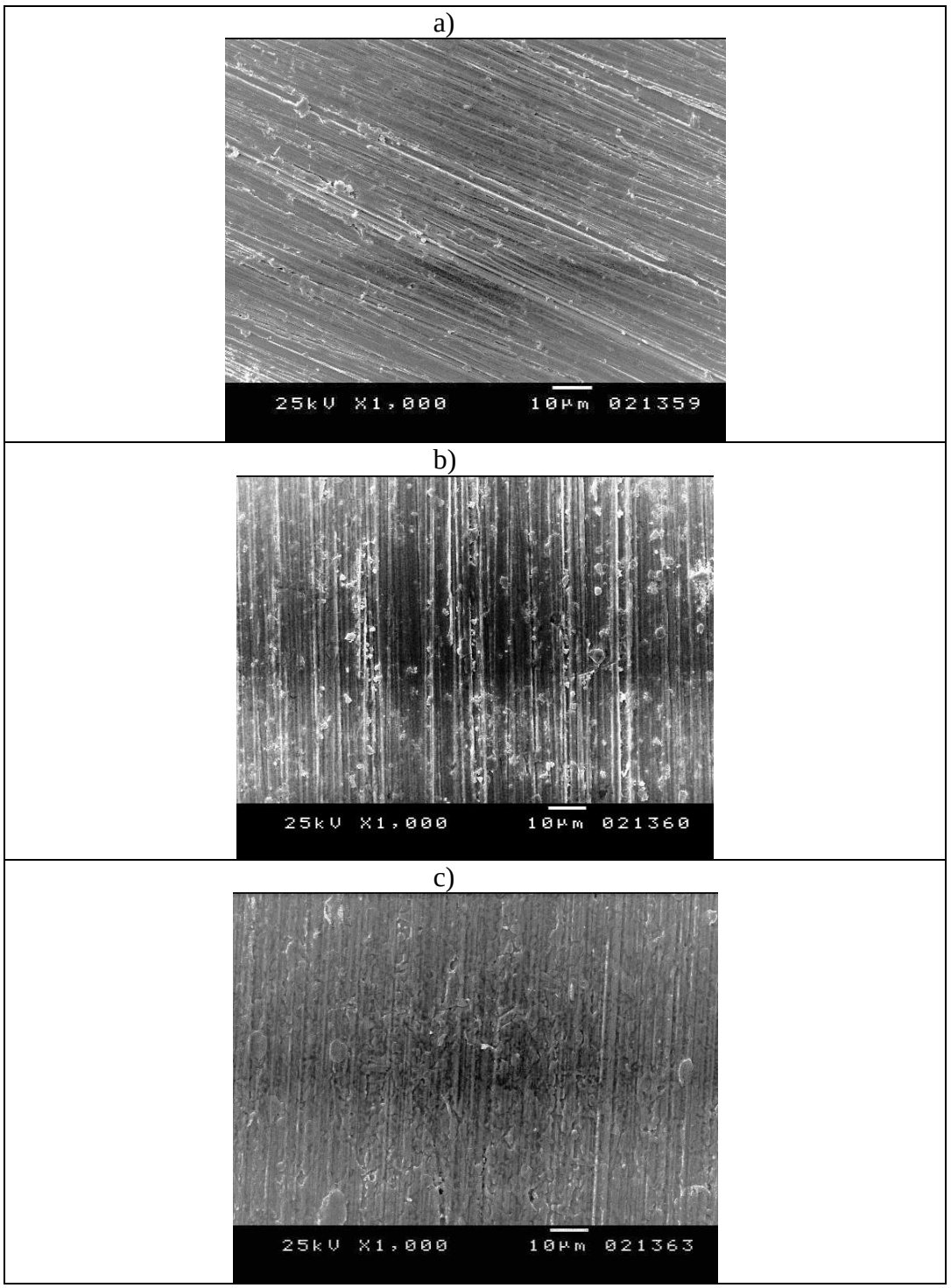

Figure 20. SEM micrographs of α-brass surface (a) before of immersion in 1 M HNO_3, (b) after 24 h of immersion in 1 M HNO_3 and (c) after 24 h of immersion in 1 M HNO_3+ 300 ppm TVE at 25 °C

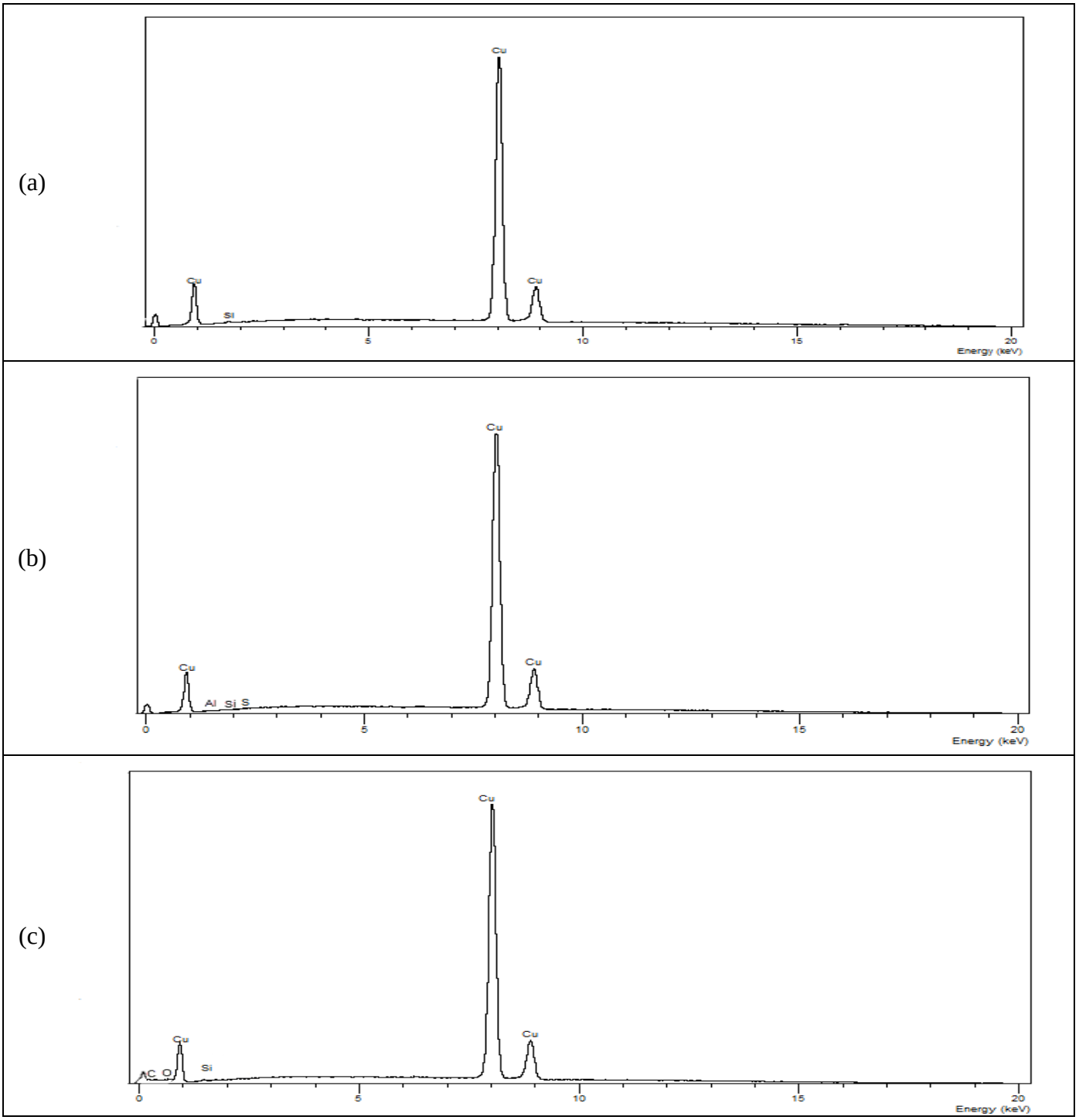

Figure 21. EDX spectra of copper surface (a) before of immersion in 1 M HNO_3, (b) after 24 h of immersion in 1 M HNO_3 and (c) after 24 h of immersion in 1 M HNO_3+ 300 ppm TVE at 25 °C

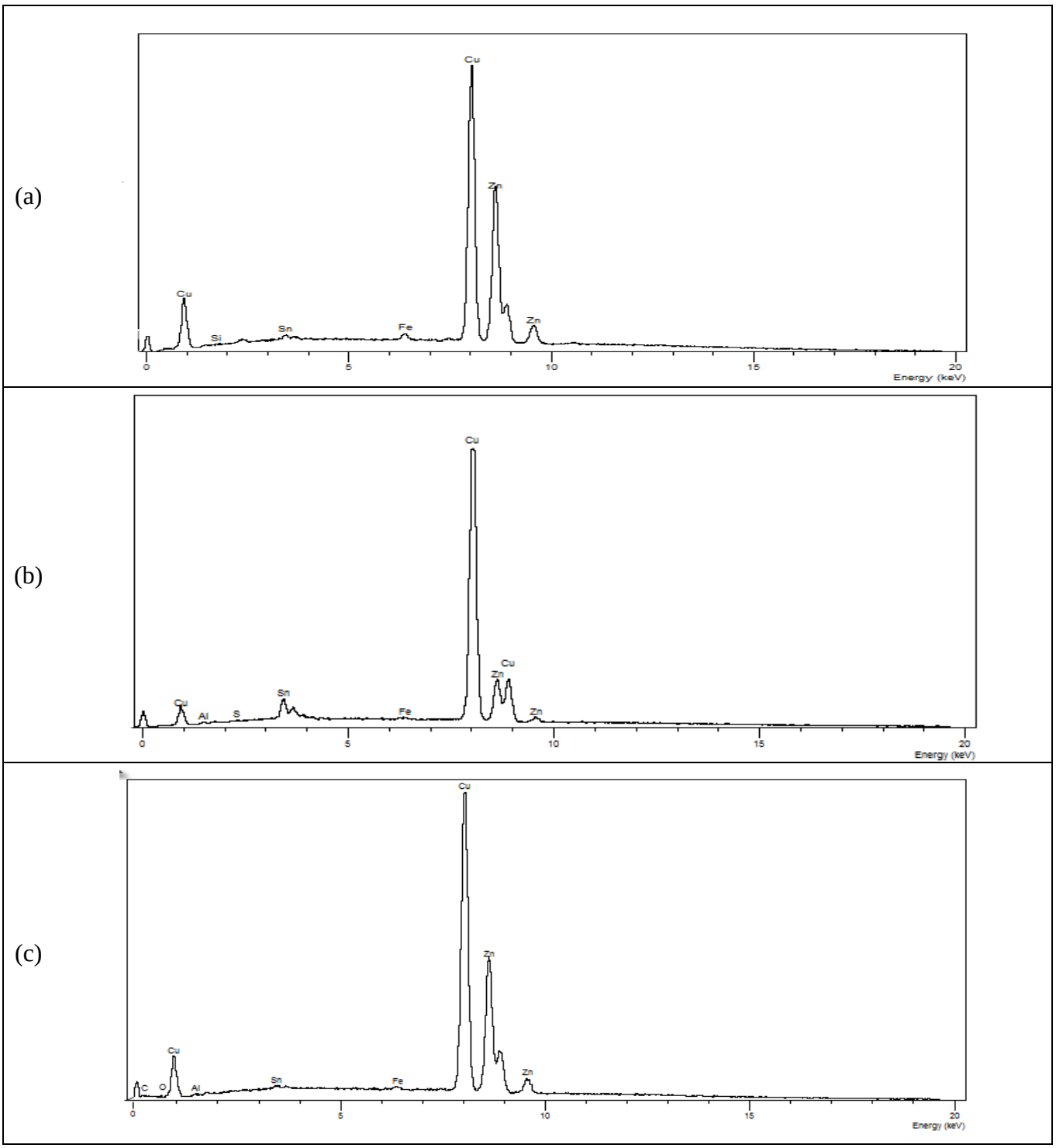

Figure 22. EDX spectra of α-brass surface (a) before of immersion in 1 M HNO_3, (b) after 24 h of immersion in 1 M HNO_3 and (c) after 24 h of immersion in 1 M HNO_3+ 300 ppm TVE at 25 °C

Table 9. Surface composition (wt %) of copper and α-bass before and after immersion in 1 M HNO_3 without and with 300 ppm of TVE at 25°C

	(Mass %)	Cu	Zn	Si	S	Fe	Al	Sn	C	O
Copper	Copper alone	99.6	--	0.4	--	--	--	--	--	--
	blank	98.9	--	0.5	0.3	--	0.3	--	--	--
	blank + 300 ppm TVE	99.4	--	0.3	--	--	--	--	0.2	0.1
α-Brass	α-Brass alone	63.4	34.4	0.3	--	1.1	0	0.8	--	--
	blank	62.8	34.1	--	0.5	0.9	0.4	1.3	--	--
	blank + 300 ppm TVE	63.1	34.2	--	--	1.0	0.3	0.9	0.3	0.2

References

1. S. Kertit, H. Essoufi, B. Hammouti, M. Benkaddour, *Chim. Phys*. 95 (1998) 2070.
2. R. Karpagavalli, S. Rajeswari, *Anti-corr. Meth. and Mat*. 45 (1998) 333.
3. W.A. Badawy, F.M. Al-kharafi, *Corros. Sci*. 55 (1999) 268.
4. M.I. Abbas, *Br. Corr. J*. 26 (1991) 273.
5. S. Kertit, B. Hammouti, *Appl. Surf. Sci*. 93 (1996) 59.
6. S.S. El-Egamy, A.S. El-Azeb, W.A. Badawy, *Corros. Sci*. 50 (1994) 468.
7. S. El Issami, L. Bazzi, M. Mihit, M. Hilali, R. Salghi, E. Ait Addi, *Physique IV* 123 (2003) 307.
8. Y. Abed, Z. Anaz, B. Hammouti, A. Aouinti, S. Kertit, A. Mansri, *J. Chim. Phys*. 96 (1999) 96.
9. S.N. Banerjee, An introduction to science of corrosion and its inhibition", Oxanian Press, New Delhi, 1985; p.286
10. K.F. Khaled, *Electrochim. Acta*. 54 (2009) 4345.
11. T. Kosec, D.K. Merl, I. Milošev, *Corros. Sci*. 50 (2008) 1987.
12. K. Rahmouni, N. Hajjaji, M. Keddam, A. Srhiri, H. Takenouti, *Electrochim. Acta*. 52 (2007) 7519.
13. L.M. Rodriguez-Valdez, A. Martinez-Villafane, D. Glossman-Matnik, *J. Mol. Struct. THEOCHEM.* 713 (2005) 65.
14. K. Barouni, L. Bazzi, R. Salghi, M. Mihit, B. Hammouti, A. Albourine, S. El Issami, *Mater. Lett.* 62 (2008) 3325.
15. J.S. Chauhan, *Asian J. Chem.*, 21(3) (2009) 1975.
16. T. V. Sangeetha, M. Fredimoses, *E-J. Chem,*. 8 (2011), S1.
17. F. Sílvio de Souza , C. Giacomelli , R. Simões Gonçalves, A. Spinelli, *Mater. Sci. Eng*. 32 (2012) 2436.
18. B.A. Abd-El-Nabey, A.M. Abdel-Gaber, M. E. Ali, , E. Khamis, S. El-Housseiny, *J. Electrochem. Sci.*, 8 (2013) 5851.
19. M.A. Mahmood, Z.A. Al- Dhaher, A.S. AL-Mizraqchi, *Iraqi J. Vet. Med.* 34 (2010) 85.
20. B. Cetin, S. Cakmakci, R. Cakmakci, *Turk. J. Agric. For.* 35 (2011) 145.
21. R.G. Parr, R.A. Donnelly, M. Levy, W.E. Palke, *J. Chem. Phys*. 68 (1978) 3801.
22. R.W. Bosch, J. Hubrecht, W.F. Bogaerts, B.C. Syrett, *Corrosion*. 57(2001) 60.
23. D.Q. Zhang, Q.R. Cai, X.M. He, L.X. Gao, G.S. Kim, *Mater. Chem. Phys*. 114 (2009) 612–617.
24. A.K. Singh, M.A. Quraishi, *Corros. Sci*. 52 (2010)1378.
25. K. K. Ai-Neami, A. K. Mohamed, I. M. Kenawy and A. S. Fouda, *Monatsh Chem.*, 126 (1995) 369.
26. K.F. Khaled, M.A. Amin, N.A. Al-Mobarak, *Appl. Electrochem*. 40 (2010) 601.
27. K.F. Khaled, S.A. Fadl-Allah, B. Hammouti, *Mater. Chem. Phys*. 117 (2009) 148.
28. G.B. Ateya, B. El-Anadouli, F. El-Nizamy, *Corros. Sci*. 24 (1984) 509.

29. M. Kliskic, J. Radosevic, S. Gndic; *J. Appl. Electrochem*. 27 (1997) 947.
30. A. M. S. Abdel, A.El- Saied, *Trans.Soc. Adv. Electrochem. Sci. Technol*. 16 (1981)197.
31. A.J. Bard, L.R. Faulkner, *Electrochemical Method, John Wiley&Sons*, NY(1980).
32. F.M. Donahue, K. Nobe, *J. Electrochem. Soc*. 112 (1965) 886.
33. E. Kamis, F. Belluci, R.M. Latanision, E.S.H. El-Ashry, *Corrosion*. 47 (1991) 677.
34. T.P. Zhao, G.N. Mu, *Corros. Sci*. 41(1999) 1937.
35. A. Döner, G. Kardas, *Corros. Sci*. 53 (2011) 4223.
36. B.G. Ateya, B.E. El-Anadouli, F.M. El-Nizamy, *Corros. Sci*. 24 (1984) 509.
37. X.H. Li, S.D. Deng, H. Fu, G.N. Mu, *Corros. Sci*. 52 (2010) 1167.
38. G. Quartarone, G. Moretti, T. Bellomi, G. Capobianco, A. Zingales, *Corrosion*. 54 (1998) 606.
39. W.D. Bjorndahl, K. Nobe, *Corrosion.* 40 (1984) 82.
40. A. Schumacher, W. Muller, Stockel, *J., Electroanal. Chem*. 219 (1987) 311.
41. D.C. Silverman, J.E. Carrico, *Corrosion*. 44 (1988) 280.
42. W.J. Lorenz, F. Mansfeld, *Corros. Sci*. 21 (1981) 647.
43. D.D. Macdonald, M.C. Mckubre, Impedance measurements in Electrochemical systems, Modern Aspects of Electrochemistry, Vol. 14, Plenum Press, New York, 1982, p. 61
44. F. Mansfeld, *Corrosion*, 36 (1981) 301.
45. C. Gabrielli, Identification of Electrochemical processes by Frequency Response Analysis, Solarton Instrumentation Group, 1980.
46. M. El Achouri, S. Kertit, H.M. Gouttaya, B. Nciri, Y. Bensouda, L. Perez, M.R. Infante, K. Elkacemi, *Prog. Org. Coat*. 43 (2001) 267.
47. J.R. Macdonald, W.B. Johanson, Theory in Impedance Spectroscopy, John Wiley& Sons, New York, 1987.
48. S.F. Mertens, C. Xhoffer, B.C. Decooman, E. Temmerman, *Corrosion*. 53 (1997) 381.
49. Trabanelli, G., Montecelli, C., Grassi, V., Frignani, A., *J. Cem. Concr. Res*., 35 (2005) 1804.
50. A.J. Trowsdate, B. Noble, S.J. Haris, I.S.R. Gibbins, G.E. Thomson, G.C. Wood, *Corros. Sci*., 38 (1996) 177.
51. F.M. Reis, H.G. de Melo, I. Costa, *J. Electrochim. Acta*. 51(2006) 1780.
52. M. Lagrenee, B. Mernari, M. Bouanis, M. Traisnel, F. Bentiss, *Corros. Sci*. 44(2002) 573.
53. E. McCafferty, N. Hackerman, *J. Electrochem. Soc*. 119 (1972) 146.
54. S.S. Abdel–Rehim, K.F. Khaled, N.S. Abd–Elshafi, *Electrochim. Acta*. 51 (2006) 3269.
55. R.R. Anand, R.M. Hurd, N. Hackerman, *J. Electrochem. Soc*. 112(1965) 138.
56. E.L. Cook, N. Hackerman, *J. Phys. Chem*. 55 (1951) 549.
57. J.J. Bordeaux, N. Hackerman, *J. Phys. Chem*. 61 (1957) 1323.
58. B.A. Abdul sattar, A.M. Hassan, A.S. Hassan, Ibn Al-Haitham *J. Pure Appl. Sci*., 25 (2012) 2.
59. A.K. Singh, M.A. Quraishi, *Corros. Sci*. 52 **(**2010) 1529.